

# Rheological fingerprinting of gastropod pedal mucus and bioinspired complex fluids for adhesive locomotion

Randy Ewoldt,<sup>a</sup> Christian Clasen,<sup>b</sup> A. E. Hosoi<sup>a</sup> and Gareth H. McKinley<sup>\*a</sup>

Receipt/Acceptance Data [DO NOT ALTER/DELETE THIS TEXT]

5 Publication data [DO NOT ALTER/DELETE THIS TEXT]

DOI: 10.1039/b000000x [DO NOT ALTER/DELETE THIS TEXT]

Nonlinear rheological properties are often relevant in understanding a material's response to its intended environment, e.g. the physiological or processing conditions of soft condensed matter. Many gastropods crawl on a thin layer of pedal mucus gel using a technique called adhesive locomotion. Adhesive locomotion (of snails or mechanical crawlers) imposes large amplitude pulsatile simple shear flow onto the supporting complex fluid, motivating the characterization of nonlinear rheological properties with large amplitude oscillatory shear (LAOS). This paper compares the rheological fingerprint of native pedal mucus with two bioinspired slime simulants, a carbomer-based polymer gel and a clay-based colloidal gel, in the context of adhesive locomotion of a mechanical system. Native slime is found to exhibit a pronounced strain-stiffening response, which is not imitated by either simulant. The most important property for optimal inclined locomotion is a large, reversible yield stress, followed by a short thixotropic restructuring time.

## 1. Introduction

Many gastropods, such as snails and slugs, crawl using a technique called adhesive locomotion, in which a thin layer (typically 10-20 μm) of excreted mucus serves both as glue and lubricant<sup>1, 2</sup>, allowing the animals to climb walls and crawl across ceilings. These gastropods exert shear stresses on this thin layer of structurally sensitive mucus that holds the organism to the substrate. The pedal mucus has an effective yield stress; at high applied stresses the network structure breaks, enabling the foot to glide forward over a fluid layer; whereas in regions of low applied stress the network structure reforms into a solid-like layer connecting the foot to the substrate (Figure 1). Gastropod pedal mucus films are physically crosslinked gels containing 0.3-9.9% (by weight) solid matter in water.<sup>3</sup> The solid constituent which dominates the mechanical properties is a mucus protein-polysaccharide complex. The glycoconjugates present in pedal mucus share similarities with both mucin glycoproteins and glycosaminoglycans in vertebrates.<sup>3</sup>

A mechanical crawler has recently been constructed which crawls using adhesive locomotion.<sup>4</sup> The success of the mechanical crawler depends critically on both the mechanical design of the robot and the rheological properties of the slime simulant. Here we compare the rheological properties of natural pedal mucus from terrestrial gastropods with two bioinspired slime simulants that have been employed as adhesives by the mechanical crawler. The first is a polymeric gel based on the carbomer Carbopol 940 and the second is a colloidal gel based on the synthetic clay LaponiteRD.

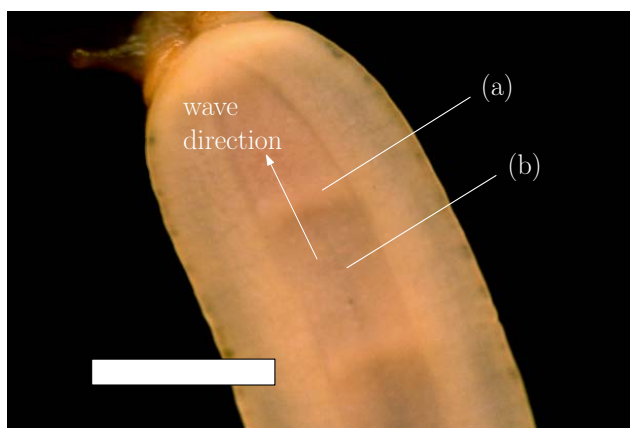


**Figure 1** Bottom view of a crawling terrestrial slug *Limax maximus*, 1cm scale bar; a) muscular contractions compress the foot parallel to the substrate, creating an area of high shear stress which ruptures the mucus network structure; b) an interwave of low stress allows the network structure to reform into a solid-like material which holds the organism to the substrate. Compression waves move toward the head (top of picture) during locomotion.

Carbopol 940 is a high molecular weight carbomer (a polymer of acrylic acid) used to modify the rheology of a variety of personal care products. LaponiteRD is a disc-shaped colloidal particle measuring approximately 300 Å in diameter and 10 Å in thickness.<sup>5</sup> Laponite clay particles form a fractal network when mixed with water at sufficient concentration.<sup>6</sup> If the colloidal dispersion is properly filtered, however, it forms a colloidal glass.<sup>7</sup>

With steady-state flow viscosity tests we show that both slime simulants satisfy a minimum yield stress criteria needed for wall climbing. In addition, we demonstrate that the linear viscoelastic behavior at low strain amplitudes of both simulants is similar to native slime. However, adhesive locomotion imposes large stresses and strains upon the material, and thus the nonlinear rheological response of slime

<sup>a</sup> MIT, Department of Mechanical Engineering, Hatsopoulos Microfluids Laboratory, Cambridge, MA, 02139 USA. E-mail: gareth@mit.edu

<sup>b</sup> University of Hamburg, Institute of Technical and Macromolecular Chemistry, 22041 Hamburg, Germany.

† Electronic Supplementary Information (ESI) available: [details of any supplementary information available should be included here]. See <http://dx.doi.org/10.1039/b000000x/>

is relevant to the dynamics of adhesive crawling. The relevant conditions for characterizing the mucin gel and simulants is large amplitude oscillatory shear (LAOS), and our measurements show that the mechanical response leading up to yield is different for the simulants compared to native slug slime; the native slime exhibits a strain-stiffening response as observed with Lissajous curves, and neither simulant mimics this.

## 2. Experimental

Pedal mucus was collected from the terrestrial snail *Helix aspera* and the terrestrial slug *Limax maximus*. A single animal was removed from the containment area, placed on a glass plate, and allowed to crawl toward a piece of food such as lettuce or a carrot. No mucus was collected until the gastropod had travelled a minimum of one body length so that no debris from the containment area remained in the sample, and to help ensure that locomotive mucus was present, rather than adhesive mucus which has been shown in some cases to have different compositional and mechanical properties.<sup>8</sup> Deposited trail mucus was gathered by scraping with a razor blade behind the crawling animal until an adequate sample size was obtained. The sample was immediately deposited on the Peltier plate of a rheometer for testing.

Carbopol 940 was obtained from the Noveon corporation (Cleveland, OH). Slime simulants based on Carbopol were prepared at various concentrations ranging from 0.5% – 4% (w/w), where w/w refers to weight of the additive with respect to the total weight of the mixture. The polymer was obtained as a white powder, and was added to deionized water being agitated with a magnetic stirrer. Samples were mixed for a minimum of 30 minutes. The Carbopol-water mixtures initially have a pH near 3, and each was neutralized with NaOH to achieve a pH=7, which produces a clear gel. The rheology of Carbopol mixtures depends on the pH, with maximum thickening occurring within a pH range of 5-9.<sup>9</sup> Carbopol dispersions are typically interpreted as microgels<sup>10, 11</sup>, in which crosslinked polymer particles are formed and swell in water. The outside of each particle exposes dangling ends which overlap with the dangling ends of other particles above a critical concentration, producing a sample-spanning network structure.

LaponiteRD was obtained from Rockwood Specialties Group, Inc. (Princeton, NJ). Simulants based on Laponite were prepared at concentrations ranging from 1% – 7% (w/w). Dispersions were prepared by adding Laponite powder to deionized water being agitated with a magnetic stirrer. Samples were mixed for 30 minutes, centrifuged, and degassed to remove air bubbles. In all cases a clear solution was formed. Laponite dispersions were brought to pH=10 by addition of NaOH to make them chemically stable.<sup>12</sup> Dispersions were kept in a sealed container and allowed to rest for a minimum of 6 hours before testing.

Rheological measurements were performed with stress-controlled AR1000-N and AR-G2 rheometers, and a strain-controlled ARES-LS rheometer (all TA Instruments, New Castle, DE). Samples were tested between both plate-plate and cone-plate geometries. For plate-plate geometries,

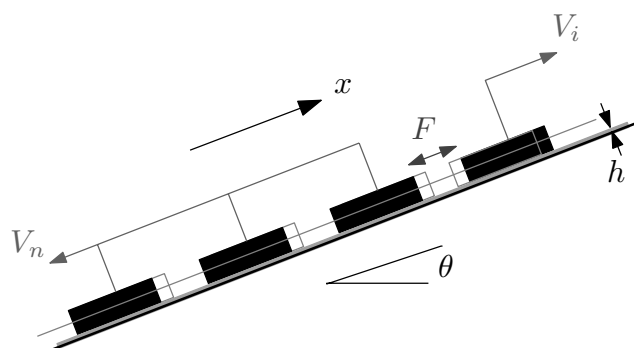


**Figure 2** Simple model of an adhesive locomotion system – the crawler consists of  $N$  discrete pads and rests on a fluid with thickness  $h$ . A controlled force iteratively moves one pad forward with respect to the rest.

diameters ranged from 0.8cm to 4cm, and gaps ranged from 200 $\mu\text{m}$  to 1000 $\mu\text{m}$ . When necessary, adhesive-backed waterproof sandpaper (2000 grit, Eastwood Co., Pottstown, PA) was attached to the top and bottom plates to help avoid slip at the boundaries. Cone-plate geometries were used for low viscosity Laponite mixtures. Two cones were used; a 4cm 2 $^\circ$  cone with 57  $\mu\text{m}$  truncation and a 6cm 1 $^\circ$  cone with 28  $\mu\text{m}$  truncation. All samples were tested at  $T=22^\circ\text{C}$ . Immediately before testing, Laponite samples were subjected to a controlled pre-shear at a shear rate  $\dot{\gamma} = 5 \text{ s}^{-1}$  for 25 seconds, followed by three minutes of recovery. The pre-shear and recovery sequence helped to erase strain history and sample loading effects, as Laponite is known to be thixotropic and to exhibit rheological aging, even under quiescent conditions.<sup>6</sup>

## 3. Results and discussion

### 3.1. Slime Simulant Requirements

A simple model is used to determine which fluid properties are desired for adhesive locomotion. The model consists of discrete pads actuated by an internal force (Figure 12), which may be interpreted as a discrete form of gastropod locomotion or a generalized model of Chan's Robosnail II.<sup>4</sup> The crawler rests on a layer of fluid, and a controlled actuator force  $F$  separates one pad away from the rest, while the rest are rigidly connected. The controlled force might come from muscles in real gastropods or from the actuators of a mechanical crawler.

It can be shown that adhesive locomotion requires, at a minimum, a non-Newtonian fluid viscosity.<sup>13</sup> Here we consider the case of idealized inclined locomotion. If the crawler is to passively keep its place on an inclined surface, yet move forward while attempting to crawl, the fluid must exhibit a rheologically-reversible apparent yield stress. This is a specific form of the rheoreversibility discussed by Carretti et al.<sup>14</sup>; the material for this application must regain its solid-like properties at low stress without the need to change environmental variables such as temperature or pH. A rheologically-reversible yield stress is characteristic of weak gels, as opposed to strong gels.<sup>15</sup> While strong gels are solid-like and may rupture at a critical stress, they do not flow above the rupture stress, nor do they regain their solid-like

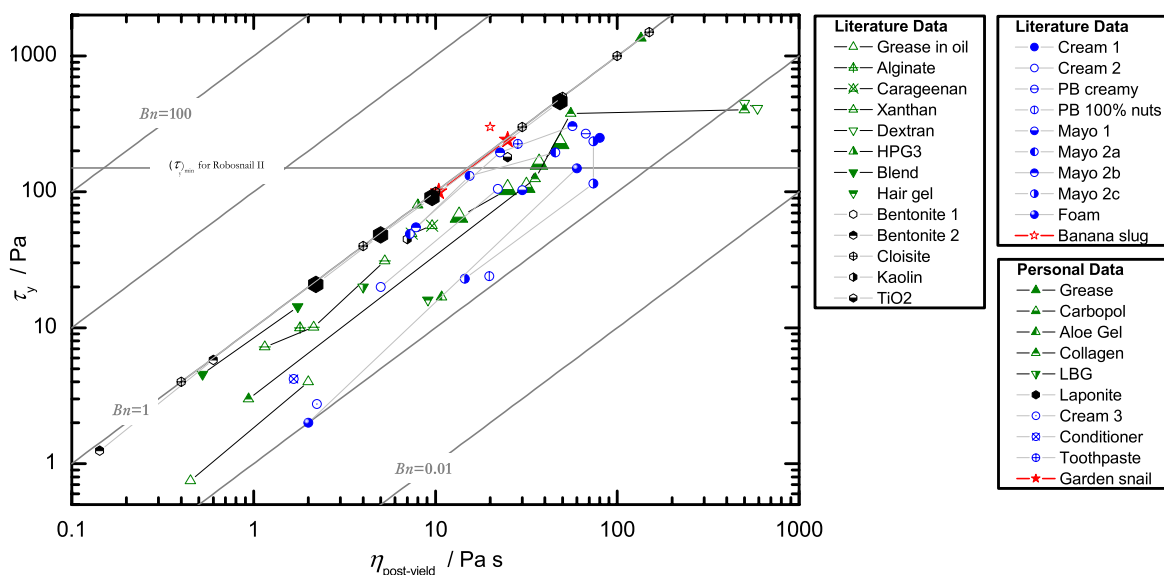


**Figure 3** Material selection space comparing yield stress fluids. A suitable simulant will meet a minimum yield stress requirement and have a low post-yield viscosity. See Electronic Supplemental Information (ESI) for material preparation and reference details.

160 nature when the stress is removed. For example, gelatin ruptures above a critical stress, but the temperature must be cycled for the pieces to recombine into a unified solid.

Inclined adhesive locomotion requires a minimum yield stress. A minimum *static* yield stress is required for the crawler to rest on an inclined surface is  $\tau_y \approx Mg \sin \theta / A$ , where  $A$  is the total contact area. The minimum yield stress required to move forward, however, is higher than the minimum static yield stress. Consider a crawler with total contact area  $A$ , consisting of  $N$  pads (Figure 12), each bearing an equal portion of the total weight  $Mg$ , traversing a surface inclined at an angle  $\theta$  with the horizontal. The discrete pad model can be generalized with  $\phi = 1/N$ , which represents the fraction of the crawler which is moving forward during actuation. If the crawler is connected to the substrate with a complex fluid having a yield stress  $\tau_y$ , then to move forward a minimum actuation force must support the pad weight and exceed the yield stress,  $F_{\min} = \phi Mg \sin \theta + \tau_y \phi A$ . The force can not be too large, however, or the rearward-tending pads will also cause the fluid under them to yield. The maximum actuating force is then expressed as  $F_{\max} = \tau_y (1 - \phi) A - Mg \sin \theta (1 - \phi)$ . When these two forces are equal, the crawler is unable to make progress since all pads would yield simultaneously. This critical point, at which  $F_{\min} = F_{\max}$ , can be recast in terms of a minimum dynamic yield stress which is required for locomotion, given by  $\tau_{y, \min} = \frac{Mg \sin \theta}{A} \left[ \frac{1}{1 - 2\phi} \right]$ . The minimum dynamic yield stress is therefore a factor of  $1/(1 - 2\phi)$  larger than the static yield stress. This can be used as a design criteria when choosing a slime simulant. For example, with Robosnail II, which has five pads, the required locomotive yield stress is approximately 67% higher than the necessary static yield stress for inclined locomotion.

Once the forward-tending pad has yielded the fluid, the speed of the crawler is inversely proportional to the flow viscosity. The center of mass velocity is  $V_{cm} = hF / A\eta$ , assuming purely viscous flow and a crawler mass equally distributed among the pads. Thus, another material property to be considered for optimization is the post-yield viscosity, which should be minimized to increase the speed of the crawler.

200 The final property considered here is the restructuring time required for the sheared fluid to regain its yield stress. This time dependent character of viscometric material functions in which structure breaks down during flow and builds up during rest is known as thixotropy.<sup>16</sup> This finite restructuring time imposes limits on the maximum velocity of an adhesive locomotion crawler. After moving a portion of its foot forward, a crawler must wait for the material to regain an adequate yield stress before actuating the next portion. Thus, the restructuring time should be minimized to increase crawler speed.

It should be noted that living gastropods may optimize pedal mucus properties with respect to an alternative cost

$$(\tau_y)_{\min} = \frac{Mg \sin \theta}{A} \left[ \frac{1}{1 - 2\phi} \right]. \quad (1)$$

function, since the organisms must expend significant energy to produce the mucus<sup>17, 18</sup>, unlike a mechanical crawler.

215 Figure 13 is a nomogram that represents candidate slime simulants in terms of two of the important fluid properties: yield stress and post-yield viscosity; for clarity the restructuring time is not shown in this two-dimensional projection. Post-yield viscosity values are taken at a shear

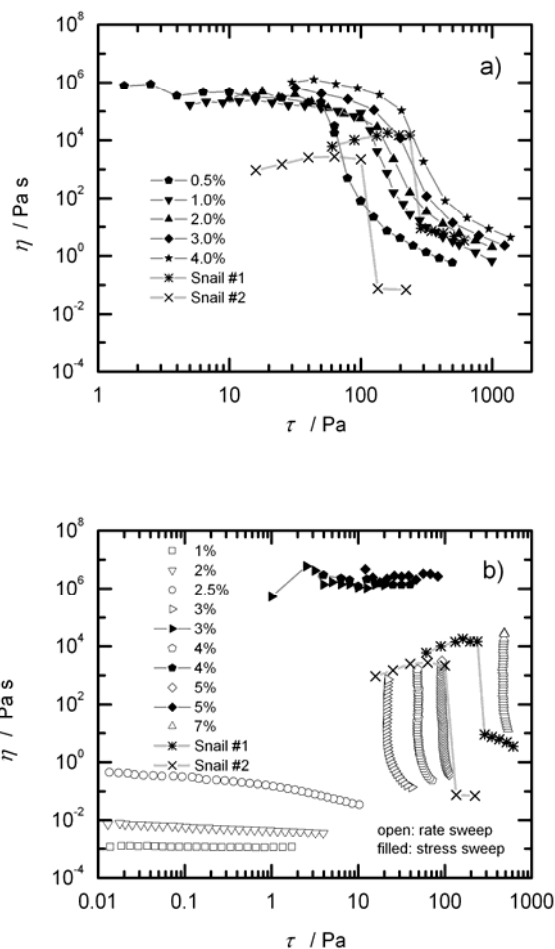


**Figure 4** Steady shear viscosity of simulants compared to native pedal mucus from *Helix aspera*; native slime collected from two snails, tested with plate-plate fixtures  $D=0.8$  mm with sandpaper,  $h=100$   $\mu\text{m}$ ; a) Carbopol-based simulant, plate-plate with sandpaper, solvent trap,  $h=1000$   $\mu\text{m}$ ,  $D=4$  cm for 0.5%-2%,  $D=2$  cm for 3%-4%; b) Laponite-based simulant, solvent trap,  $D=6$  cm  $1^\circ$  cone-plate for 1%-2%,  $D=4$  cm  $2^\circ$  cone-plate for 2.5%,  $D=4$  cm plate-plate,  $h=1000$   $\mu\text{m}$  with sandpaper for 3%-7%.

rate  $\dot{\gamma}=10$   $\text{s}^{-1}$ , which is a representative shear rate for Robosnail II, since the pad velocity is  $V_i \approx 1$   $\text{cm}\cdot\text{s}^{-1}$  and the fluid thickness is  $h \approx 1$  mm. A line of minimum locomotive yield stress for vertical wall climbing can be drawn for Robosnail II, such that any simulant below this line will not meet the criteria for vertical wall climbing. Lines of constant Bingham number are plotted on the figure as a guide to the eye. The Bingham number is motivated by the Bingham model for a yield stress fluid<sup>19</sup>, and is given by  $Bn = \tau_y / \eta \dot{\gamma}$ , where  $\tau_y$  is the yield stress,  $\eta$  is the viscosity, and  $\dot{\gamma}$  is the shear rate, again  $\dot{\gamma}=10$   $\text{s}^{-1}$  for the plot to be consistent with the post-yield viscosity data. For the case of a vertical climber the Bingham number represents a comparative measure of support forces and resistive forces, therefore high  $Bn$  is desirable.

It can be seen from Figure 13 that there are slime simulants which meet the minimum criteria for a wall climbing mechanical crawler that uses adhesive locomotion. Thus,

although native slug slime could be used for a mechanical crawler, harvesting slime is not required to operate a mechanical wall climbing device. Furthermore, the minimum required yield stress scales as weight over area, and therefore scales as the characteristic length of the crawler,  $\tau_y \propto Mg/A \propto L$ . Thus, for a similar aspect ratio a smaller crawler will require a lower yield stress and more fluids will be available for use.

### 3.2. Rheological Material Functions

Two promising slime simulants, the particulate gel based on Laponite and the polymer gel based on Carbopol, were examined in detail and compared with native pedal mucus from the terrestrial snail *Helix aspera* and the terrestrial slug *Limax maximus*.

#### 3.2.1. Steady shear flow

The steady shear viscosity of the Carbopol-based and Laponite-based simulants and native pedal mucus from *Helix aspera* are shown in Figure 14. Data is shown for two different samples of pedal mucus. At sufficient concentration, each material exhibits a dramatic increase in the viscosity at low stresses. The viscosity for these materials is so high that it is solid-like for timescales on the order of seconds, which is the relevant timescale of locomotion for natural gastropods<sup>20</sup> and for Chan's mechanical crawler. For example, with a viscosity  $\eta \approx 10^6$  Pa.s, and a fluid thickness  $h=1$  mm, Chan's crawler would slump down a vertical wall at a rate of only 0.3  $\text{mm}\cdot\text{hr}^{-1}$ . At a critical stress the high viscosity decreases by several decades. Since flow exists for any finite stress, none of these materials exhibits a true yield stress. However, this behavior may be described as an apparent yield stress, since the flow at low applied stresses may be difficult to observe, and it is followed by a dramatic drop in viscosity over a narrow range of stress. The critical stress at which viscosity dramatically changes will henceforth be referred to as the yield stress<sup>21, 22</sup>.

Native slime and the Laponite gel share a steep and dramatic drop in viscosity at the yield stress (Figure 14b), whereas the viscosity of the Carbopol solutions drop less quickly as stress is increased (Figure 14a). The drop in viscosity of Laponite occurs over such a narrow range of stress that a stress-sweep could not capture the behavior. Thus, a rate-sweep was performed from high shear-rates down to low shear-rates. This technique allows for large changes in viscosity to be measured over a small change in stress. A stress-sweep was used to explore the high viscosity region of the flow curve, since the data was beyond the experimental range of the rate-sweep.

Each of these materials is rheologically reversible, so that solid-like properties are regained when the stress is reduced below the yield stress, and the test can be repeated to give the same data. The timescale over which the material restructures is known as the thixotropic timescale<sup>16</sup>, which may affect the value of the measured yield stress<sup>23</sup>; this will be discussed further in Section 3.2.4.

The data for both simulants show that the yield stress is a strong function of concentration. The maximum yield stress

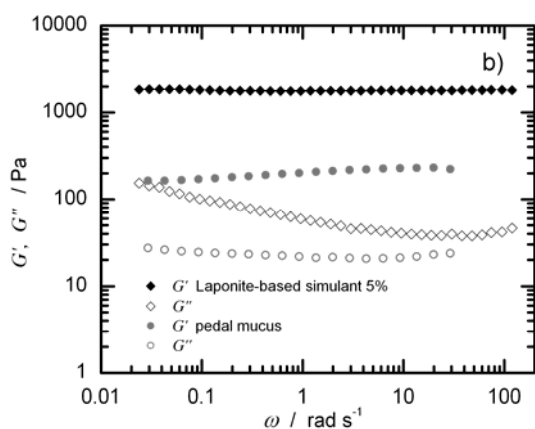
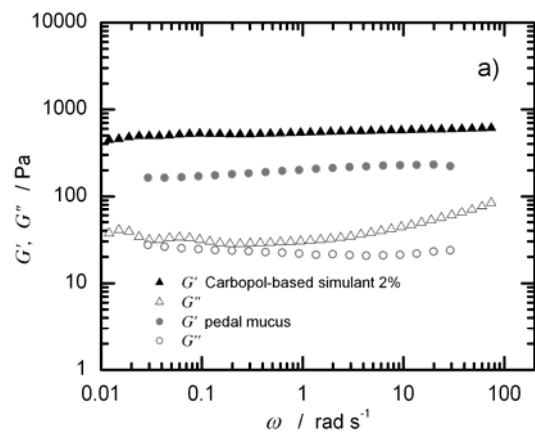


**Figure 5** Linear viscoelastic moduli of simulants compared with native pedal mucus from *Limax maximus*; pedal mucus tested with  $D=2$  cm plate with sandpaper, solvent trap,  $h=200$   $\mu\text{m}$ ,  $\tau_0=5$  Pa; simulants tested with  $D=4$  cm plate with sandpaper,  $h=1000$   $\mu\text{m}$ , solvent trap; a) Carbopol-based simulant,  $\tau_0=5$  Pa; b) Laponite-based simulant,  $\tau_0=20$  Pa

of each simulant is limited by the impracticality of increasing the concentration beyond a certain point. Extremely high yield stress materials are also difficult to test, since they suffer from slip at the boundaries.<sup>24</sup> Wall slip can be witnessed by observing the edge of the sample during the test<sup>25</sup>; this method indicates that Laponite at 7% is prone to slippage at the boundary. Thus, the data reported in Figure 14b give the apparent viscosity for a gap  $h = 1000$   $\mu\text{m}$ ; if slip is occurring then the measured viscosity will be a function of gap height.<sup>26</sup>

### 3.2.2. Linear Viscoelasticity

The linear viscoelasticity of the materials was examined with small amplitude oscillatory shear (SAOS). The native slime is compared here to simulants which have similar yield stress values: a Carbopol-based simulant at 2% and a Laponite-based simulant at 5%, each having a yield stress  $\tau_y \approx 100$  Pa. The linear rheological regime is defined such that the material properties are not a function of the input stress amplitude, and thus each oscillation test in the linear regime is performed below the yield stress ( $\tau_0 \ll \tau_y$ ).

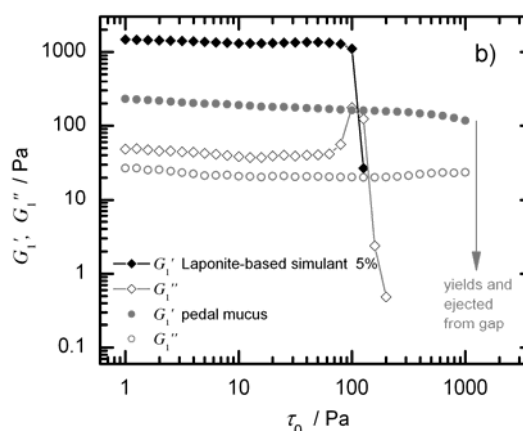
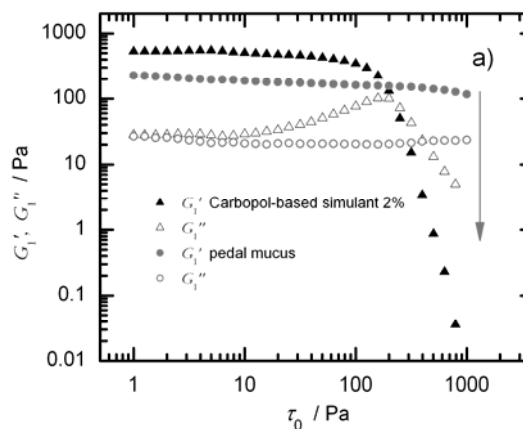


**Figure 6** Large amplitude oscillatory shear (LAOS) of simulants compared with native pedal mucus from *Limax maximus*, same geometries as Figure 15, all samples tested at  $\omega=1$   $\text{rad}\cdot\text{s}^{-1}$ ; a) Carbopol-based simulant; b) Laponite-based simulant.

The linear viscoelastic moduli,  $G'$  and  $G''$ , were examined over a range of frequencies using SAOS. Both the elastic and viscous contribution to the complex modulus were found to be weak functions of frequency for each sample below the yield stress, as shown in Figure 15. Although each material has approximately the same yield stress, the storage moduli vary over an order of magnitude; native slime has the lowest elastic modulus, near 200 Pa, whereas the Laponite has a storage modulus  $G' \approx 2000$  Pa. Thus, although the yield stress is comparable, the elastic stiffness of the particulate gel simulant (Figure 15b) is a factor of ten larger than native slime.

### 3.2.3. Large Amplitude Oscillatory Shear (LAOS)

A crawling slug subjects the pedal mucus film to shear stresses that exceed the yield stress, and thus the large amplitude, nonlinear viscoelastic properties of both native slime and slime simulants are relevant in adhesive locomotion. The shear stress exerted by a crawling slug can exceed 2000 Pa, as measured by Denny.<sup>20</sup> Furthermore, the strain amplitude under a crawling slug can be estimated from the speed versus time profile reported by Denny.<sup>20</sup> Using this data, and assuming the pedal mucus thickness  $h = 20$   $\mu\text{m}$ , a

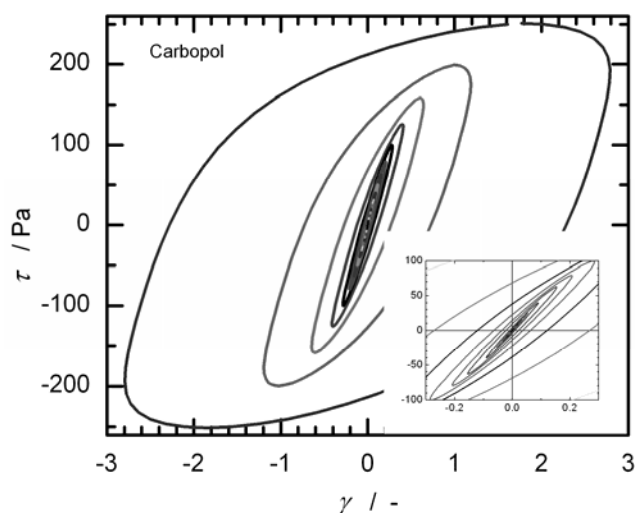


**Figure 7** Lissajous curves resulting from the large amplitude oscillatory shear tests shown in Figure 16a for the polymer gel simulant.

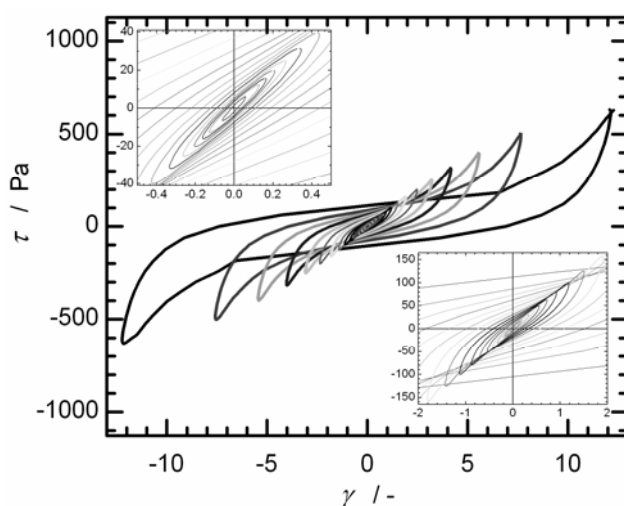


**Figure 9** Lissajous curves resulting from the large amplitude oscillatory shear tests shown in Figure 16 for native pedal mucus from *Limax maximus*.

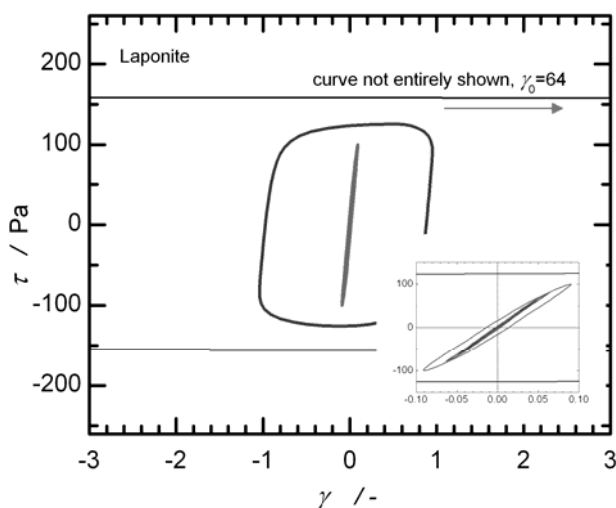


**Figure 8** Lissajous curves resulting from the large amplitude oscillatory shear tests shown in Figure 16b for the particulate gel simulant.

strain  $\gamma \sim O(10^2)$  is imposed on the pedal mucus with each pulsatile wave.

The response of a material to oscillatory shear is considered nonlinear if the storage and loss moduli depend on the input stress (or strain) amplitude. Additionally, the strain (or stress) response may be observed to contain higher harmonics than the input frequency, rather than exhibiting a pure harmonic response. In this nonlinear case the linear moduli  $G'$  and  $G''$  are not uniquely defined. The response can be analyzed with a Fourier transform<sup>27</sup>, and the real and imaginary coefficients of the higher harmonic contributions can be represented as  $G_n'$  and  $G_n''$  respectively. To be precise, we will therefore report the first harmonic elastic and loss moduli,  $G_1'$  and  $G_1''$ , for LAOS results, which reduce to  $G'$  and  $G''$  in the linear regime.

The first harmonic of the storage modulus  $G_1'$  and loss modulus  $G_1''$  are shown in Figure 16 as a function of stress amplitude  $\tau_0$  at a fixed frequency of  $\omega = 1 \text{ rad.s}^{-1}$ . At low stresses each material shows little or no dependence on the

input stress amplitude. Each material undergoes a transition at a critical stress at which the elastic response dramatically decreases. However, no data could be collected for native slime beyond this critical stress since the material was ejected from the gap. The critical stress amplitude for this transition corresponds approximately to the apparent yield stress in steady flow tests (Figure 14). The sharpness of the transition also corresponds with the steady shear flow results; the polymer gel simulant exhibits a gentle stress softening, whereas the slime and particulate gel simulant show a very sharp transition at a critical stress.

The critical yield strain may be expected to obey the relationship  $\tau_y \sim G\gamma_y$  where  $G$  is the nominal elastic modulus of the material. This is approximately true for the simulants. The yield stresses are similar and the elastic modulus of the Laponite gel is approximately three times that of the Carbopol. This difference in elastic modulus is therefore compensated by changes in the critical strain. The critical yield strain for the particulate gel Laponite is smaller (by approximately six times) than the polymer-based Carbopol gel. The particulate-based material requires a smaller strain to distort the microstructure out of equilibrium.

As the stress amplitude approaches the yield stress, a minor difference can be seen in the behavior of  $G_1'$  and  $G_1''$  for each material. The loss modulus  $G_1''$  appears to increase just before yield for each material; this increase is most pronounced with the Carbopol simulant. The increase in  $G_1''$  prior to yield, combined with a decrease in  $G_1'$ , has been observed in other materials and is classified as type III LAOS behavior by Hyun and coworkers.<sup>28</sup> The variation of the first harmonic storage modulus is less interesting as the yield stress is approached; in each case  $G_1'$  is a weak function of stress amplitude for  $\tau_0 < \tau_y$ . However, upon closer inspection, a dramatic difference in the material response leading up to failure becomes apparent.

With the aid of a Lissajous curve one can immediately see the substantial difference in each material's non-linear response to an oscillatory stress input, as demonstrated in

Figure 7, Figure 8, and Figure 9. These Lissajous curves are parametric plots of stress upon strain, with each curve corresponding to an oscillatory shear test with a sinusoidal stress input at a particular frequency and amplitude. The trajectory is elliptic for a linear viscoelastic material, approaching the limiting case of a straight line for a Hookean elastic solid and an ellipse with axes aligned to the coordinates for a Newtonian fluid. A nonlinear, non-sinusoid material response will distort the ellipse. The cyclic integral of a Lissajous curve, in which stress is plotted against strain, is equal to the energy dissipated per unit volume per cycle,  $E_d$ , and is directly related to the loss modulus  $G_1''$  as  $E_d = \gamma_0^2 \pi G_1''$ .<sup>29</sup>

The Lissajous curves of each material at low stress appear as tight ellipses (see insets in Figure 17, Figure 18, and Figure 19) indicating  $G' \gg G''$ ; only a small area is enclosed and the response is dominated by elasticity. As the imposed stress amplitude is increased toward the yield stress each material exhibits distinctive behavior. The Laponite simulant maintains tight ellipse curves almost all the way up to yield, and subsequently undergoes a quick transition to predominantly viscous behavior, as shown by a dramatic increase in the area enclosed by the curve. This transition is consistent with the sudden drop in viscosity for the steady state flow curves (Figure 14b). The Lissajous curves for the Carbopol (Figure 7) gradually broaden to enclose more area, and thus show a gradual transition from elastic to viscous behavior. This soft transition is consistent with the steady state flow tests (Figure 14a) and the behavior of  $G_1'$  and  $G_1''$  as the oscillatory stress amplitude is increased (Figure 16a).

In contrast to the two simulants, the native pedal mucus exhibits a strongly nonlinear response leading up to yield. For native slime the elliptical curves which are present at low stresses become progressively distorted as the stress amplitude is increased. The distortion is such that the stress increases sharply at large strains. This upturn in stress can be interpreted as a form of strain-stiffening, since the maximum stress is higher than would be expected if the small strain response were fit to an ellipse and projected to large strains. It is significant to note that this nonlinear response is not captured by monitoring  $G_1'$ , as shown in Figure 16, in which  $G_1'$  of native slime is a very weak function of stress amplitude. The strain-stiffening reported for native slime is not mimicked by either of the Carbopol or Laponite gel simulants.

### 3.2.4 Time dependency of yield stress

The apparent yield stress of a material is likely to depend on how long the sample has been at rest since it was last yielded, i.e. there is a timescale of restructuring (thixotropy) to regain the yield stress nature of the material.<sup>16, 23</sup> Furthermore, the maximum velocity of a mechanical crawler is inversely related to the restructuring time.<sup>13</sup>

The restructuring times of Carbopol and Laponite gel simulants were examined using shear stress overshoot tests.<sup>30</sup> The sample is first shear rejuvenated, or pre-sheared, to yield the material and erase any strain history effects. The pre-shear is abruptly brought to a halt, at which point the sample is allowed to age for a waiting time  $t_w$ . A step-strain-rate is

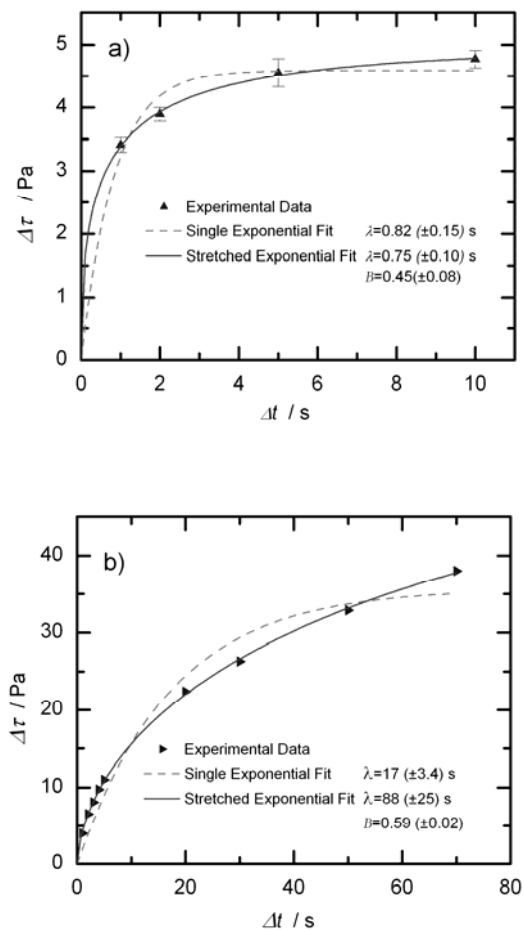


**Figure 10** Time-dependent stress overshoot of simulants,  $D=5 \text{ cm } 1^\circ$  cone-plate; a) Carbopol 2%, error bars shown at one standard deviation; b) Laponite 3%

then imposed, which yields the sample. The resulting overshoot stress  $\Delta\tau$  is then determined as the difference between the peak shear stress and the steady flow stress, and is expected to depend on the time  $t_w$  that the microstructure has been allowed to equilibrate. The overshoot stress is not quantitatively equivalent to the yield stress as defined in this work. However, it is closely correlated to the yield stress, as it is the peak stress which occurs as the strain is increased and the material microstructure is ruptured.

The results of time-dependent overshoot tests for the simulants are shown in Figure 20. The Laponite sample (3%) was pre-sheared at  $\dot{\gamma} = 5 \text{ s}^{-1}$  for 60 seconds. Less shearing was needed to eliminate strain history effects with the Carbopol, which was pre-sheared at  $\dot{\gamma} = 5 \text{ s}^{-1}$  for five seconds. Each was allowed to rest for a specified time and then sheared at  $\dot{\gamma} = 5 \text{ s}^{-1}$ . Error bars are shown for the Carbopol data since each test was repeated three times. The minimum waiting time allowed by the rheometer is one second.

An appropriate form of the rheological aging observed in the samples is a stretched exponential approach to an asymptotic value observed at long rest times

**Table 1** Summary of rheological properties of two simulants with similar apparent yield stresses compared with native gastropod pedal mucus

	Native pedal mucus	Carbomer-based simulant (polymer gel)	Clay-based simulant (particulate gel)
Yield stress	100 - 240 Pa	108 Pa	90.8 Pa
Post-yield viscosity, $\eta$ ( $\dot{\gamma} = 10 \text{ s}^{-1}$ )	10.4 - 25 Pa.s	31.6 Pa.s	9.6 Pa.s
$G'$ ( $\omega = 1 \text{ rad.s}^{-1}$ )	200 Pa	540 Pa	1800 Pa
$G''$ ( $\omega = 1 \text{ rad.s}^{-1}$ )	20 Pa	30 Pa	60 Pa
Yield stress transition	Sharp	Soft	Sharp
Pre-yield stiffening	Yes	No	No
Single exponential restructuring time, $\lambda$	0.85 s [adapted <sup>33</sup> ]	0.8 s	17 s

where  $\Delta\tau_{\infty}$  is the maximum overshoot stress at long rest times,  $t_w$  is the rest time,  $\lambda$  is the characteristic restructuring time, and  $B$  is the stretching exponent. Stretched exponentials have been observed with numerous systems and have been associated with the presence of fractal networks.<sup>31</sup> When  $B=1$ , Equation (4) represents a single exponential aging timescale, which has previously been associated with the aging of the yield stress.<sup>32</sup> Each data set in Figure 20 has been fitted to Eq (4) as both a single exponential ( $B=1$ ) and a stretched exponential. Fitting results are shown in Figure 20.

For a yield stress that grows in a similar fashion to Equation (4), the restructuring time  $\lambda$  is inversely related to the maximum velocity of a mechanical crawler.<sup>13</sup> The polymer gel has a much faster restructuring time than the particulate gel. The single exponential restructuring timescale of Carbopol is  $\lambda \approx 0.8 \text{ s}$ , whereas the restructuring time of Laponite is  $\lambda \approx 17 \text{ s}$ . Thus, the maximum velocity of a mechanical crawler on Carbopol would be approximately 20 times that of a crawler on Laponite. The stretched exponential timescales are also dramatically different.

Denny has performed similar overshoot tests with gastropod pedal mucus, and found the peak stress as a function of wait time could be fit to a power law.<sup>33</sup> A single exponential timescale can be fit to the first ten seconds of this power law giving  $\lambda \approx 0.85 \text{ s}$  with  $R^2=0.74$ . Thus pedal mucus and the Carbopol simulant share similar restructuring times.

#### 4. Conclusions

It has been known for some time that pedal mucus from terrestrial gastropods exhibits a yield stress<sup>2</sup>, but the present work is the first examination of the progressive transition from an elastic gelled solid to a nonlinear viscoelastic fluid as the oscillatory shear stress amplitude is increased. Lissajous curves (such as Figure 19) can be used to graphically indicate the observed strain-stiffening behavior of native pedal mucus. The bulk rheological response of native slime was used as a benchmark for comparing two possible complex fluids (a

$$\Delta\tau(t_w, \dot{\gamma}) = \Delta\tau_{\infty}(\dot{\gamma}) \left( 1 - e^{-(t_w/\lambda)^B} \right) \quad (2)$$

particulate gel and a polymeric gel) for the purpose of enabling mechanical adhesive locomotion.

A large number of structured materials were surveyed as possible slime simulants, including polymer gels, particulate gels, emulsions, wet foams, and composites (Figure 13). Two

simulants which could be formulated to have similar yield stresses to that of native slime (Figure 14) were then chosen for further study. When examined in detail, in linear and nonlinear deformation, the simulants show some differences in rheological properties. Table 1 summarizes the results of the comparison of these simulants with native gastropod pedal mucus.

The three key parameters for a complex fluid to be useful in adhesive locomotion are a high yield stress,  $\tau_y$ , to support the crawler on an inclined surface, a low post yield viscosity,  $\eta$ , to increase speed, and a small restructuring timescale,  $\lambda$ , also to increase speed. Of the two simulants analyzed in this work, the Carbopol-based polymer gel is the best candidate for use in adhesive locomotion. It provides sufficient yield stress, a moderate post-yield viscosity, and a restructuring time that is more than an order of magnitude smaller than the Laponite-based colloidal gel simulant. Native pedal mucus, however, is still better than the best simulant; pedal mucus provides a similar yield stress and restructuring time, but with a lower post-yield viscosity.

A more general scientific question related to this work is how to characterize soft condensed matter in relevant conditions. One aspect of relevant characterization is the length scale of interest. It is noteworthy that no rheological measurements have been reported for native pedal mucus at the physiologically relevant gap thickness  $h=10-20 \mu\text{m}$ , including the results presented here. Most tests are reported with a gap height one to two orders of magnitude larger than this, and it is possible that native pedal mucus acts differently in a confined space.

The type of rheological test performed must also be relevant to the material's intended use. Linear viscoelasticity is robust (in the linear regime), but may not fully apply to the intended use of the material. In this work, nonlinear rheological tests revealed properties such as oscillatory yield stress, oscillatory yield strain, restructuring time, the nature of the yield transition, and strain-stiffening in native slime. However, this strain-stiffening could not be observed with the common measures of nonlinear viscoelasticity ( $G_1'$  and  $G_1''$ ), but was instead revealed by plotting the raw data as Lissajous curves. A suitable quantitative measure might also be devised to reveal this behaviour in the future. There exist other ways to characterize nonlinear rheology, such as the quantitative measures of nonlinearity suggested by Tee and Dealy<sup>34</sup>, or the differential modulus devised by Gardel et al.<sup>35</sup> to describe actin networks. The differential modulus is measured while subjecting the material to a prestress, and is therefore readily used with elastically dominated systems, but may be less



robust for softer, more lossy materials which are dominated by flow. In general, when a material of interest is exposed to large stresses or strains in its environment, the nonlinear rheological properties will be significant, and one must decide which tests and measures are relevant to the intended use of the material.

## Notes and references

‡ Footnotes should appear here.

1. M. W. Denny, *Nature*, 1980, **285**, 160-161.
2. M. W. Denny and J. M. Gosline, *J. Exp. Biol.*, 1980, **88**, 375-393.
3. M. W. Denny, in *The Molluska*, ed. P. W. Hochachka, 1983, vol. 1. Metabolic Biochemistry and Molecular Biomechanics, pp. 431-465.
4. B. Chan, N. J. Balmforth and A. E. Hosoi, *Phys. Fluids A*, 2005, **17**, 113101.
5. A. Mourchid, A. Delville, J. Lambard, E. Lecolier and P. Levitz, *Langmuir*, 1995, **11**, 1942-1950.
6. F. Pignon, A. Magnin, J. M. Piau, B. Cabane, P. Lindner and O. Diat, *Phys. Rev. E*, 1997, **56**, 3281-3289.
7. D. Bonn, H. Kellay, H. Tanaka, G. Wegdam and J. Meunier, *Langmuir*, 1999, **15**, 7534-7536.
8. A. M. Smith and M. C. Morin, *Biol. Bull.*, 2002, **203**, 338-346.
9. Noveon, in *TDS 237*, <http://www.personalcare.noveon.com/techdata/Carbopo1980.asp>, 1998.
10. N. W. Taylor and E. B. Bagley, *J. Appl. Polym. Sci.*, 1974, **18**, 2747-2761.
11. J. O. Carnali and M. S. Naser, *Colloid Polym. Sci.*, 1992, **270**, 183-193.
12. A. Mourchid, E. Lecolier, H. Van Damme and P. Levitz, *Langmuir*, 1998, **14**, 4718-4723.
13. R. Ewoldt, M.S. Thesis, Massachusetts Institute of Technology, 2006.
14. E. Carretti, L. Dei and R. G. Weiss, *Soft Matter*, 2005, **1**, 17-22.
15. S. B. Ross-Murphy, *J. Rheol.*, 1995, **39**, 1451-1463.
16. H. A. Barnes, *J. Non-Newtonian Fluid Mech.*, 1997, **70**, 1-33.
17. M. Denny, *Science*, 1980, **208**, 1288-1290.
18. E. Lauga and A. E. Hosoi, *Phys. Fluids A*, 2006, to appear.
19. R. Bird, R. Armstrong and O. Hassager, *Dynamics of Polymeric Liquids*, 2nd edn., John Wiley & Sons, Inc, New York, 1987.
20. M. W. Denny, *J. Exp. Biol.*, 1981, **91**, 195-217.
21. H. A. Barnes, *J. Non-Newtonian Fluid Mech.*, 1999, **81**, 133-178.
22. H. A. Barnes and K. Walters, *Rheol. Acta*, 1985, **24**, 323-326.
23. P. C. F. Moller, J. Mewis and D. Bonn, *Soft Matter*, 2006, **2**, 274-283.
24. H. A. Barnes, *J. Non-Newtonian Fluid Mech.*, 1995, **56**, 221-251.
25. D. M. Kalyon, P. Yaras, B. Aral and U. Yilmazer, *J. Rheol.*, 1993, **37**, 35-53.
26. A. Yoshimura and R. K. Prudhomme, *J. Rheol.*, 1988, **32**, 53-67.
27. M. Wilhelm, *Macromol. Mater. Eng.*, 2002, **287**, 83-105.
28. K. Hyun, S. H. Kim, K. H. Ahn and S. J. Lee, *J. Non-Newtonian Fluid Mech.*, 2002, **107**, 51-65.
29. S. N. Ganeriwala and C. A. Rotz, *Polym. Eng. Sci.*, 1987, **27**, 165-178.
30. S. M. Fielding, P. Sollich and M. E. Cates, *J. Rheol.*, 2000, **44**, 323-369.
31. J. R. Macdonald and J. C. Phillips, *J. Chem. Phys.*, 2005, **122**, 074510.
32. L. Heymann, E. Noack, L. Kaempfe and B. Beckmann, Proceedings of the XXIIth International Congress on Rheology, Laval University, Quebec City (Quebec), Canada, 1996.
33. M. W. Denny, *American Zoologist*, 1984, **24**, 23-36.
34. T. T. Tee and J. M. Dealy, *Transactions of the Society of Rheology*, 1975, **19**, 595-615.
35. M. L. Gardel, J. H. Shin, F. C. MacKintosh, L. Mahadevan, P. Matsudaira and D. A. Weitz, *Science*, 2004, **304**, 1301-1305.